

Computationally efficient method for Fourier transform of highly chirped pulses for laser and parametric amplifier modeling

ALEXEY ANDRIANOV,^{1,*} ARON SZABO,² ALEXANDER SERGEEV,¹
ARKADY KIM,¹ VLADIMIR CHVYKOV,² AND MIKHAIL KALASHNIKOV^{2,3}

¹*Institute of Applied Physics of the Russian Academy of Sciences, 603950 Nizhny Novgorod, Russia*

²*ELI-Hu Nkft., Dugonics ter 13, H-6720 Szeged, Hungary*

³*Max-Born-Institut für Nonlinear Optics and Short Pulse Spectroscopy, Max-Born-Strasse 2a, 12489 Berlin, Germany*

*alex.v.andrianov@gmail.com

Abstract: We developed an improved approach to calculate the Fourier transform of signals with arbitrary large quadratic phase which can be efficiently implemented in numerical simulations utilizing Fast Fourier transform. The proposed algorithm significantly reduces the computational cost of Fourier transform of a highly chirped and stretched pulse by splitting it into two separate transforms of almost transform limited pulses, thereby reducing the required grid size roughly by a factor of the pulse stretching. The application of our improved Fourier transform algorithm in the split-step method for numerical modeling of CPA and OPCPA shows excellent agreement with standard algorithms.

© 2016 Optical Society of America

OCIS codes: (190.5530) Pulse propagation and temporal solitons; (000.3860) Mathematical methods in physics; (190.4970) Parametric oscillators and amplifiers; (140.4480) Optical amplifiers; (320.1590) Chirping; (320.5520) Pulse compression.

References and links

1. G. P. Agarwal, *Nonlinear Fiber Optics (Fourth Edition)* (Academic, San Diego, 2006).
2. J. O. Smith, *Mathematics of the Discrete Fourier Transform (DFT)* (W3K Publishing, 2007).
3. I. Epatko, A. A. Malyutin, R. V. Serov, D. Solov'ev, and A. Chulkin, "New algorithm for numerical simulation of the propagation of laser radiation," *Quantum Electron.* **28**(8), 697 (1998).
4. O. Morice, "Miró: complete modeling and software for pulse amplification and propagation in high-power laser systems," *Opt. Engineering* **42**(6), 1530–1541 (2003).
5. B. Jaskorzynska, J. Nilsson, A. Sergeev, and E. Vanin, "Time-frame transformation for efficient simulation of chirped pulse compression in an optical fiber," *Opt. Lett.*, **20**(20), 2123–2124 (1995).
6. H. M. Ozaktas, M. A. Kutay, and Z. Zalevsky, *The Fractional Fourier Transform: with Applications in Optics and Signal Processing* (Wiley, Chichester, 2001).
7. W.L. Katw, "Phase-Sensitive Amplification of Pulses in Nonlinear Optical Fibers", in book *Computational Wave Propagation*, T.Hagstrom, B. Engquist, G.A.Kriegsmann, eds. (Springer-Verlag New York, 1996).
8. S. N. Vlasov, E. V. Kuposova, and G. I. Freidman, "Interaction of frequency-modulated light beams in multistage parametric amplifiers at the maximum gain bandwidth," *Quantum Electron.* **39**(5), 393 (2009).
9. A. Andrianov, E. Anashkina, A. Kim, I. Meyerov, S. Lebedev, A. Sergeev, and G. Mourou, "Three-dimensional modeling of cpa to the multimillijoule level in tapered Yb-doped fibers for coherent combining systems," *Opt. Express* **22**(23), 28256–28269 (2014).
10. N. Didenko, A. Konyashchenko, A. Lutsenko, and S. Y. Tenyakov, "Contrast degradation in a chirped-pulse amplifier due to generation of prepulses by postpulses," *Opt. Express* **16**(5), 3178–3190 (2008).
11. D. Schimpf, E. Seise, J. Limpert, and A. Tunnermann, "The impact of spectral modulations on the contrast of pulses of nonlinear chirped-pulse amplification systems," *Opt. Express* **16**(14), 10664–10674 (2008).
12. X. Liu, A. P. Shreenath, M. Kimmel, R. Trebino, A. V. Smith, and S. Link, "Numerical simulations of optical parametric amplification cross-correlation frequency-resolved optical gating," *J. Opt. Soc. Am. B* **23**(2), 318–325 (2006).
13. J. Wang, P. Yuan, J. Ma, Y. Wang, G. Xie, and L. Qian, "Surface-reflection-initiated pulse-contrast degradation in an optical parametric chirped-pulse amplifier," *Opt. Express* **21**(13), 15580–15594 (2013).

1. Introduction

Optical pulses with a large quadratic phase (frequency chirp) in the temporal or spatial domain appear in many fields of linear and nonlinear optics. For example, the chirped pulse amplification (CPA) technique utilizes large time-stretched pulses by propagating the pulse through a dispersive medium where the pulse acquires large phase with a leading quadratic term in the corresponding Taylor expansion. Similarly beam diffraction and focusing requires the consideration of spatial phase distributions with large leading quadratic term. Numerical modeling of the propagation of highly chirped pulses in a nonlinear amplifying media is important in the development of ultrashort pulse high-power laser systems. Numerical methods for modeling pulse propagation, e.g., the well-known split-step method [1] extensively use fast Fourier transform (FFT). Spectral and temporal profiles must fit the FFT grid in order to avoid an aliasing effect. Consequently, high levels of pulse chirping require the number of grid points roughly to be rescaled by the factor of stretching. Comprehensive modeling of modern CPAs and optical parametric chirped pulse amplifiers (OPCPA) with large stretching factors of $10^4 - 10^6$ (femtosecond to nanosecond duration) usually requires enormous grid size when considering transverse beam distributions using standard split-step propagation methods.

This letter presents an advanced new method for Fourier transform calculation that largely relaxes requirements for grid size and allows straightforward extension of FFT-based beam propagation algorithms for pulses with arbitrary large stretching factors. This development enables the efficient modeling of nonlinear 3-D beam propagation with commercial desktop computers. The paper starts with reviewing the difficulties in applying FFT to highly chirped pulses, followed by the derivation of the modified transformation formula which can be used to compute efficiently Fourier transform of highly chirped pulses. Finally the modified transformation used to simulate nonlinear CPA and OPCPA systems with a 10^4 fold reduction of computational time and memory consumption for typical parameters.

2. Advanced Fourier transform for chirped pulses

The forward Fourier transform of the function $A(t)$ from the temporal (t) to the frequency (ω) domain is given by operator \hat{F}

$$\hat{F}[A](\omega) = \frac{1}{\sqrt{2\pi}} \int_{-\infty}^{\infty} A(t) \exp(i\omega t) dt. \quad (1)$$

The backward transform is given by inverse operator \hat{F}^{-1} and has the same form as (1) where ω and t are interchanged and i is replaced by $-i$.

In numerical implementations, the finite-dimensional version of the above transform, when applied to a discretized function $A_m = A(m\Delta t)$ produces a discretized spectrum $\tilde{A}_m \approx \hat{F}[A](m\Delta\omega)$, where $m = 1..N$, Δt is the time discretization step, $\Delta\omega = 2\pi/N\Delta t$ is the frequency discretization step and N is the number of the grid points. To obtain meaningful results, both the temporal $A(t)$ and spectral A_ω distributions have to be sufficiently small outside the computational windows in time domain ($N\Delta t$) and in frequency domain ($N\Delta\omega$).

We introduce a chirped pulse with the spectrum $B_\omega = A_\omega \exp(i\psi(\omega))$, where A_ω is the Fourier transform of its original complex amplitude $A(t)$ (before chirping) and $\psi(\omega)$ is the spectral phase produced by the stretcher with leading term $\alpha\omega^2/2$ in its Taylor expansion. An attempt to compute the temporal shape of the stretched pulse with large chirp factor α by using FFT may produce incorrect result due to the "aliasing" or "folding" effect of FFT [2]. Folding becomes important if the phase difference in the frequency domain between two adjacent nodes exceeds π or if the stretched pulse in time domain becomes longer than the grid size $N\Delta t$ (see Fig. 1).

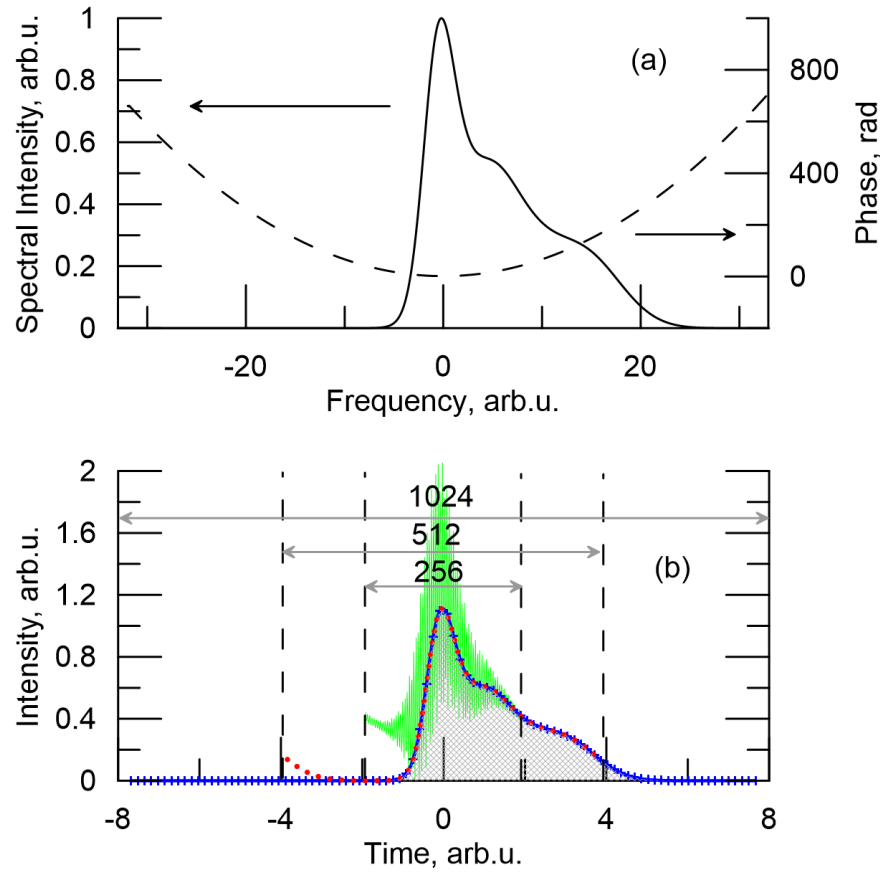


Fig. 1. Folding effect of FFT: (a) chirped pulse spectral intensity (solid line) and spectral phase (dashed line), (b) inverse Fourier transforms computed by standard FFT with grid sizes 256 (green line), 512 (dotted red line), 1024 (blue solid line with crosses), and by our modified transform with grid size 256 (filled gray curve). Temporal grid sizes are shown by dashed vertical lines.

In previous works, methods based on the Talanov transformation (“lens transformation”) of the propagation equation were proposed to reduce required grid size and were successfully used in some numerical implementations in space and time domains (see [3–5] and references therein). It was also pointed out that the fractional Fourier transform [6] can be used in the numerical modeling of chirped pulse propagation [7], however, this direction was not further developed to the best of our knowledge. Our efficient method for Fourier transform of highly chirped pulses is mathematically exact and does not require transformation of the propagation equation, thus in combination with the standard split-step algorithm it offers a universal simulation tool for arbitrary propagation distances and initial linear chirps.

The new algorithm is obtained by rewriting the spectrum of the chirped pulse from the initial $A(\omega)$ as $B_\omega = A'_\omega \exp(i\alpha\omega^2/2)$ where the quadratic phase is explicitly factored out. The high order phase terms induced by the stretcher are included in the modified spectral amplitude $A'_\omega = A_\omega \exp(i\psi(\omega) - i\alpha\omega^2/2)$ and the related backward Fourier transform $A'(t) = \hat{F}^{-1}[A'_\omega](t)$ consequently has a slightly different duration than the initial pulse $A(t)$. This is significantly shorter than the duration of the stretched pulse. The temporal profile of the stretched pulse to be computed is given by backward Fourier transform $B(T) = \hat{F}^{-1}[B_\omega](T) =$

$\hat{F}^{-1}[\hat{F}[A'(t)](\omega) \exp(i\alpha\omega^2/2)](T)$. The latter expression can be written explicitly in the form of double integral

$$B(T) = \frac{1}{2\pi} \int_{-\infty}^{\infty} \int_{-\infty}^{\infty} A'(t) \exp\left(\frac{i\alpha\omega^2}{2} + i\omega t - i\omega T\right) dt d\omega. \quad (2)$$

The integral over ω can be evaluated by changing the variable $\omega = (T - t)/\alpha + q\sqrt{2/\alpha}$:

$$\int_{-\infty}^{\infty} \exp\left(\frac{i\alpha\omega^2}{2} + i\omega(t - T)\right) d\omega = \sqrt{\frac{2}{\alpha}} \exp\left(-\frac{i(t - T)^2}{2\alpha}\right) \int_{-\infty}^{\infty} \exp(iq^2) dq = \sqrt{\frac{2i\pi}{\alpha}} \exp\left(-\frac{i(t - T)^2}{2\alpha}\right). \quad (3)$$

Thus, the following expression for $B(T)$ is obtained:

$$B(T) = \sqrt{\frac{i}{2\pi\alpha}} \exp\left(-\frac{iT^2}{2\alpha}\right) \int_{-\infty}^{\infty} A'(t) \exp\left(-\frac{it^2}{2\alpha} + \frac{itT}{\alpha}\right) dt, \quad (4)$$

where the last integral has the form of forward Fourier transform of the function $A'(t) \exp(-it^2/2\alpha)$, taken at a characteristic frequency $\Omega = T/\alpha$. By substituting $A'(t) = \hat{F}^{-1}[B_\omega \exp(-i\alpha\omega^2/2)]$ as previously introduced, we obtain

$$B(T) = \sqrt{\frac{i}{\alpha}} \exp\left(-\frac{iT^2}{2\alpha}\right) \hat{F} \left[\hat{F}^{-1} \left[B_\omega \exp\left(-\frac{i\alpha\omega^2}{2}\right) \right] (t) \exp\left(-\frac{it^2}{2\alpha}\right) \right] \left(\frac{T}{\alpha} \right). \quad (5)$$

This expression connects the spectrum of the chirped pulse B_ω and its temporal shape $B(T)$ and thus acts as a modified backward Fourier transform for chirped pulses. The most attractive feature of Eq. (5) is that both the forward and backward Fourier transforms are taken for almost transform-limited functions since the phase term $it^2/2\alpha$ is small on the time scale of $A'(t)$ and α is assumed to be large. Therefore, in numerical calculations, FFT with sufficiently small resolution and grid size can be used to accommodate $A'(t)$ which differs only slightly from the initial (unchirped) pulse. It follows from Eq. (5) that temporal resolution of stretched pulse is $\Delta T = \alpha\Delta\omega = 2\pi\alpha/N\Delta t$ and total size of the stretched temporal window is $T_\alpha = N\Delta T = 2\pi\alpha/\Delta t$, which automatically scale up with increasing chirp factor. For a given spectrum, a grid size in the frequency domain large enough to avoid clipping of spectral wings should be chosen. Also, a reasonable grid resolution is necessary to properly sample spectral intensity and phase excluding the quadratic term, i.e. $\psi(\omega) - \alpha\omega^2/2$ must be $< \pi$ between adjacent nodes.

This criterion forms the limitations of the modified transform method which arise from the fast variation of the residual phase $\psi(\omega) - \alpha\omega^2/2$. For example, if the signal is a coherent sum of two pulses with different chirp factors α_1 and α_2 , the modified method can still be applied by substituting the average value of $\bar{\alpha} = (\alpha_1 + \alpha_2)/2$ as base chirp instead of α into Eq. (5). This results in residual phases of the same absolute value but different sign for the pulses, $\pm(\alpha_1 - \alpha_2)\omega^2/4$, which must satisfy the above condition. This can be rewritten explicitly as $|\alpha_1 - \alpha_2|\Delta\omega^2 N < 4\pi$ or, equivalently, $|\alpha_1 - \alpha_2|\pi < N\Delta t^2$. Additionally, the total frequency grid size $\Delta\omega N$ must be large enough to accommodate the spectra of the pulses, and the total stretched temporal grid size must be large enough in case of large temporal separation between the pulses.

The same approach can be used to derive a modified forward Fourier transform that connects the temporal representation of $B(T)$ to its spectrum B_ω . The final result is symmetric to Eq. (5)

$$B_\omega(\omega) = \sqrt{\frac{\alpha}{i}} \exp\left(\frac{i\alpha\omega^2}{2}\right) \hat{F} \left[\hat{F}^{-1} \left[B(\alpha\Omega) \exp\left(\frac{i\alpha\Omega^2}{2}\right) \right] (t) \exp\left(\frac{it^2}{2\alpha}\right) \right] (\omega). \quad (6)$$

As a summary of the method, a 5-step algorithm, based on Eqs. (5) and (6), for computing the Fourier transforms of a highly chirped pulse can be formulated:

1. The initial field is multiplied by the exponent factor which compensates for a large quadratic phase
2. A backward FFT is applied (on almost transform-limited signal)
3. The result is multiplied by the intermediate exponent factor $\exp(it^2/2\alpha)$, adding a small quadratic phase
4. FFT is applied (again, on almost transform-limited signal)
5. The result is multiplied by the exponent factor which restores large quadratic phase.

The initial and final steps can be omitted if a large quadratic phase is implied but not explicitly present in the input data and is not explicitly required in the result. The extra cost of doubling the number of FFT calls is reasonable as the resulting large reduction in needed grid size N and computational time $N \log N$ scale according to the pulse stretching coefficient s , which is the ratio of the stretched pulse duration and the initial pulse duration. The modified transform method has smaller computational cost compared to the ordinary FFT at larger grid even for moderate stretching coefficients as $2.5 \sim 3$, depending on the particular implementation of the numerical scheme. The proposed transform is also mathematically exact as no approximation were used in the formation of Eqs. (5) and (6). This means that this approach can be applied to pulses with arbitrary large chirp.

In case of low-chirped pulses, a limitation from the folding effect may occur at step 4 in the numerical implementations arising from a large phase in the intermediate exponent. This sets the lower bound for the chirp value at which the modified transform can be used as $\alpha > N\Delta t^2/\pi$. This condition is fulfilled for commonly used parameters, which can be illustrated by considering a Gaussian pulse as a simple example with amplitude $A(t) = \exp(-t^2/2\tau^2)$, where $\tau \approx 0.6\tau_{FWHM}$ is the pulse duration. It can be shown that the stretching coefficient is $s = \sqrt{1 + \alpha^2/\tau^4}$. In numerical simulations the pulse duration is chosen to be some fraction η of the temporal grid size, i.e. $\tau = \eta N\Delta t$. Now, the above condition can be written as $\sqrt{s^2 - 1} > 1/\pi\eta^2 N$, which is fulfilled for $s > 2.5$ and usual values of $\eta \approx 0.05$ and $N > 64$.

An example of Fourier transform of a complex highly chirped pulse computed with the modified algorithm is shown in Fig. 1(b) by shaded curve.

In the following example the modified transform method was applied to pulse with very large chirp parameters $\alpha \gg \Delta\tau^2$, where $\Delta\tau$ is the characteristic timescale of the unchirped pulse. In this case, the intermediate exponential factor in Eq. (5) may be omitted and the following is obtained

$$B(T) \approx \sqrt{\frac{i}{\alpha}} \exp\left(-\frac{iT^2}{\alpha}\right) B_{\omega}\left(\frac{T}{\alpha}\right). \quad (7)$$

This equation demonstrates the well known fact that the temporal shape for pulses with a large quadratic phase mimics its spectrum. It makes clear that $\Omega = T/\alpha$ has physical meaning of instantaneous frequency at time T . The approach based on the direct connection of spectral and temporal intensities, complemented by establishing a direct connection between the instantaneous frequency and position in time for highly chirped pulses, is used for simplified treatment of nonlinear amplification of highly chirped pulse, (see [8]).

Thus, the above modified transforms provide an accurate extension of this simplified approach to pulses with arbitrary magnitude of quadratic chirp.

3. Application of the modified Fourier transform method to CPA modeling

In this section, the application of the modified Fourier transform method for numerical simulation of CPA is demonstrated. Here, a one-dimensional case, which may correspond to the amplification

of the central part of a large beam in active laser medium or amplification in a single mode optical fiber, is considered. However, a straightforward extension to a more general model (even 3-D [9]) is possible. Our model is based on the nonlinear Schrödinger equation including a laser gain term [1]

$$\frac{\partial A}{\partial z} = -\frac{i\beta_2}{2} \frac{\partial^2 A}{\partial t^2} + \frac{\beta_3}{6} \frac{\partial^3 A}{\partial t^3} + \frac{g}{2} A + i\gamma |A|^2 A, \quad (8)$$

where $\beta_2 = 42\text{ps}^2/\text{km}$ and $\beta_3 = 0.07\text{ps}^3/\text{km}$ are the 2^{nd} and 3^{rd} order dispersion coefficients, $g = 0.033\text{cm}^{-1}$ is the gain and $\gamma = 1\text{W}^{-1}\text{km}^{-1}$ is the effective nonlinearity. These are typical values for a single mode fiber at the wavelength of 1030 nm.

The initial pulse with Gaussian shape and transform-limited duration of 200 fs was stretched to about 1 ns by adding quadratic spectral phase with chirp factor $\alpha = 100\text{ps}^2$. The second order symmetric split-step method, in which dispersion and gain are treated in the spectral domain and nonlinearity in the temporal domain, was used for the numerical integration of Eq. (8). Initial numerical simulation used ordinary FFTs to switch between time and frequency domains ("basic" algorithm). A very large grid ($N = 2^{22}$) with temporal resolution $\Delta t = 15$ fs was used to avoid the folding effect for highly chirped pulses. The ordinary FFTs was replaced by corresponding modified transforms ("advanced" algorithm). A much smaller grid size of $N = 2^9$ (corresponding to temporal window size $T = 7.68$ ps) was used with the same temporal resolution (15 fs) to accommodate initial unchirped pulse. The stretched grid had resolution 81.9 ps and total size 41.72 ns. In the implementation of split-step method with modified Fourier transform steps 1. and 5. were omitted, further reducing the number of required multiplications.

Figures 2(a) and 2(b) compare the simulation results after recompression (quadratic spectral phase removal). The spectral intensity and phase results of the advanced algorithm perfectly match the basic algorithm even though they are sampled with different resolutions. The phase distortions arising from dispersion and nonlinearity (B-integral ≈ 5) are also accurately modeled by the advanced algorithm. Temporal intensity distributions distorted by nonlinearity also coincide within the modeling window. The advanced algorithm was validated with different parameters (dispersion ranging from -200 to 200 ps^2/km , symmetric and asymmetric pulse shapes, chirp factor up to 500 ps^2) and found to be in excellent agreement with the basic algorithm whilst memory consumption and computational time improved proportionally to the grid size reduction (10^4 in the demonstrated case).

The power of the advanced algorithm was demonstrated by modeling a more complex process of contrast degradation during the amplification of the pulse interacting with a small post-pulse. The only difference from the previous case is the addition of a small replica of the input pulse delayed by $\tau = 8\text{ps}$ with 10^8 times lower intensity to mimic a typical experimental situation. It was shown previously that several pulses arise before and after the main pulse at the compressor output due to the amplifier nonlinearity [10, 11]. In this case, the temporal window size was set to $T = 61.44$ ps for the advanced algorithm so that several pre- and post-pulses could be captured. This required $N = 2^{12}$ grid points which is still much less than for the basic algorithm. Figure 2(c) compares the simulation results which show once more excellent agreement and allows contrast evaluation up to 10^{20} .

4. Application of the advanced algorithm to OPCPA modeling

The advanced algorithm can be applied to the problem of OPCPA modeling, with some additional considerations. Here, a 1-D numerical model is discussed which is based on the well-known three-wave mixing equations describing nonlinear interaction, phase mismatch and dispersion. This can be used for the central part of the beam assuming negligible diffraction and walk-off [12]:

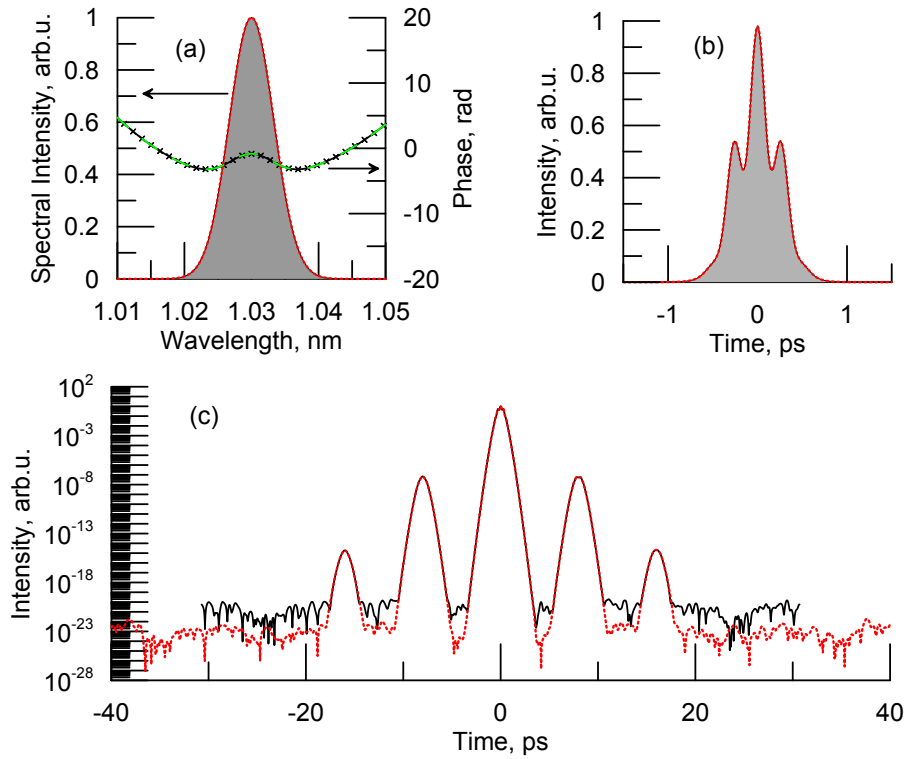


Fig. 2. The calculated CPA output: a) the Spectrum (gray shaded curve, basic algorithm; red dashed line, advanced algorithm) and spectral phase (black line with crosses, basic; green dashed line, advanced); b) The temporal profile (gray shaded curve, basic; red line, advanced); c) The temporal profile of output pulse with pre- and post-pulses (red dotted line, basic; black line, advanced).

$$\left(\frac{\partial}{\partial z} + \frac{1}{v_{s,i}} \frac{\partial}{\partial t} + \frac{i\beta_2^{s,i}}{2} \frac{\partial^2}{\partial t^2} \right) A_{s,i} = \frac{i\omega_{s,i} d_{eff}}{n_{s,i} c} A_p A_{i,s}^* e^{i\Delta k z} \quad (9)$$

$$\left(\frac{\partial}{\partial z} + \frac{1}{v_p} \frac{\partial}{\partial t} + \frac{i\beta_2^p}{2} \frac{\partial^2}{\partial t^2} \right) A_p = \frac{i\omega_p d_{eff}}{n_p c} A_s A_i e^{-i\Delta k z} \quad (10)$$

where the subscripts (s,i,p) refer to signal, idler and pump; v_j is the group velocity; β_2 is the 2nd order dispersion coefficient; d_{eff} is the effective nonlinear mixing coefficient; n_j is the refractive index; ω_j is the central frequency and Δk is the phase mismatch. Equation (9), taken with corresponding subscripts, describes the evolution of the signal and idler pulses and Eq. (10) is used for pump pulses. With high power OPCPA only a chirped signal pulse and a pump pulse (which is usually close to transform-limit) are present at the input of the nonlinear crystal. The chirp factor of the signal pulse, α is taken from parameters of the stretcher and is considered constant throughout the simulation. The initial phase of the growing idler pulse has the opposite sign to the signal (provided the pump pulse is not chirped), hence, $-\alpha$ chirp factor is used in the transforms for the idler. The pump pulse is assumed to be narrowband, so that it is most efficiently evaluated using standard FFT with the temporal grid matched to the stretched temporal grids of the signal and the idler. This leads to a smaller span of the spectral grid for the pump pulse with the same number of points and therefore has higher frequency resolution. As an example, the amplification of a 200 fs transform-limited Gaussian pulse with 800 nm central wavelength is

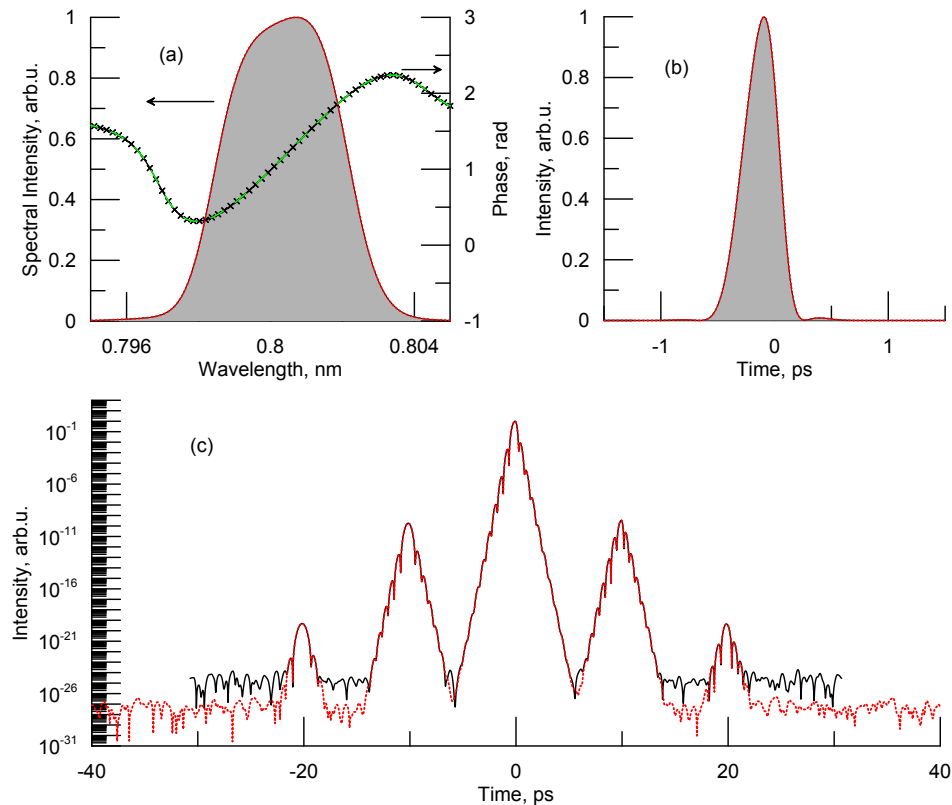


Fig. 3. The calculated OPCPA output: a) the Spectrum (gray shaded curve, basic algorithm; red dashed line, advanced algorithm) and spectral phase (black line with crosses, basic; green dashed line, advanced); b) The temporal profile (gray shaded curve, basic; red line, advanced); c) The temporal profile of output pulse with pre- and post-pulses (red dotted line, basic; black line, advanced).

modeled. The pulse was stretched to 1 ns by adding spectral phase $\phi = \alpha\omega^2/2 + \alpha_3\omega^3/6$, where $\alpha = 100 \text{ ps}^2$, and a cubic phase with coefficient $\alpha_3 = 0.01 \text{ ps}^3$ was added. The other amplifier parameters correspond to a 10 mm BBO crystal pumped by 1.5 ns Gaussian pulses with peak intensity of 0.5 GW/cm^2 at 532 nm in collinear geometry. Narrow amplification bandwidth ($\approx 4 \text{ nm}$) and saturation effects lead to noticeable distortion of the recompressed pulse.

Figures 3(a) and 3(b) show that the numerical results from basic and advanced algorithms are almost in perfect agreement. A 10^8 times smaller post-pulse, delayed by 10 ps was added to model contrast degradation due to saturation during parametric amplification [13]. There is very good agreement of the compressed pulse shapes including the fine structure and decaying pulse wings down to 10^{-22} level (see Fig. 3(c)). This proves the applicability of the advanced algorithm to contrast evaluation problems, which are of major importance for modern high intensity laser systems.

5. Conclusion

In conclusion, we have developed a new approach to calculate the Fourier transform of signals with arbitrary large quadratic phase which can be efficiently implemented in numerical simulations utilizing FFTs. The application of an advanced algorithm, utilizing the modified method of Fourier transform, to modeling CPAs and OPCPAs has been demonstrated and it

shows an excellent agreement with the basic algorithm. Our modified transform method can be widely used in numerical codes dealing with highly chirped pulses by simply replacing regular FFT calls. Upgrading to higher dimensions is straightforward and can be especially useful for modeling diffraction and focusing. There is a significant reduction in the required memory and a corresponding improvement of the computational speed for the highly demanding problems of 3-D nonlinear modeling of modern high energy CPA laser systems by using the advanced algorithm. Our test runs show that modeling OPCPA of 20 fs pulses stretched to 1 ns with reasonable transverse resolution (512x512 points, 1024 temporal points) is possible on a desktop computer with 16 GBytes RAM, while the basic algorithm requires hundreds TBytes.

Funding

This work was supported by ELI-HU Nonprofit Ltd. (Research Collaboration Agreement ELIALPS_Laser_R&D_TC3.2_IAP) and Russian Science Foundation (RSF) (16-12-10472). The ELI-ALPS project (GINOP-2.3.6-15-2015-00001) is supported by the European Union and co-financed by the European Regional Development Fund.